communications materials

A Nature Portfolio journal

Article

https://doi.org/10.1038/s43246-025-00781-8

Crosslinking substrate regulates frictional properties of tissue-engineered cartilage and chondrocyte response to loading

Christoph Meinert[1,2,9], Angus Weekes[1,3,4,9], Chun-Wei Chang[1,3], Karsten Schrobback[5], Amy Gelmi[6], Molly M. Stevens[6,7,8], Dietmar W. Hutmacher[1,3,4] & Travis J. Klein[1,4]

Hydrogels are frequently used in regenerative medicine due to their hydrated, tissue-compatible nature, and tuneable mechanics. While many strategies enable bulk mechanical modulation, little attention is given to tuning surface tribology, and its impact on cellular behavior under mechanical stimuli. Here, we demonstrate that photocrosslinking hydrogels on hydrophobic substrates leads to significant, long-lasting reductions in surface friction, ideal for cartilage tissue regeneration. Gelatin methacryloyl and hyaluronic acid methacrylate hydrogels photocrosslinked on polytetrafluoroethylene possess more hydrated, lubricious surfaces, with lower friction coefficients and crosslinking densities than those crosslinked on glass. This facilitated self-lubrication via water exudation, limiting shear during biaxial stimulation. When subject to intermittent biaxial loading mimicking joint movement, low-friction chondrocyte-laden neo-tissues formed superior hyaline cartilage, confirming the benefits of reduced friction on tissue development. Finally, in situ photocrosslinking enabled precise hydrogel formation in a full-thickness cartilage defect, highlighting the clinical potential and emphasizing the importance of crosslinking substrate in regenerative medicine.

A plethora of native biological systems rely on efficient lubrication and reduction of frictional forces to facilitate their physiological function, including the pleural cavity[1], the surface of the eye[2], visceral organs, and diarthrodial joints[3]. Disruption of lubrication and increased friction within such systems leads to progressive degeneration and loss of function[3]. This underscores the importance of achieving physiological tribological properties in engineered tissues.

A key class of biomaterials with potential for regulation of tribological properties are hydrogels, water-swollen three-dimensional (3D) polymer networks which mimic key features of native extracellular matrices. Hydrogels are regarded as excellent biomaterials for tissue engineering purposes and may be engineered to display cell-instructive cues that promote neo-tissue formation in a 3D environment[4]. As a result, hydrogels have been extensively investigated as scaffolds for the engineering of tissues such as skin[5], bone[6], muscle[7], and articular cartilage[8,9]. The cell-mediated generation of neo-tissue constructs, however, is a slow process that involves the biosynthesis and functional maturation over months to years. Thus, it is imperative that tissue engineering matrices and early developing neo-tissues possess appropriate mechanical and frictional properties that prevent wear of the bioartificial implant, while providing a cellular micro- and mechanical environment supporting tissue integration and regeneration[10]. A variety of strategies have been evaluated to improve the mechanical characteristics of hydrogels[4], primarily the compressive[11] and tensile properties[12] of this intrinsically brittle and soft class of biomaterials. Improving the tribological properties of hydrogels applied in cartilage tissue engineering, however, has been largely neglected.

Both intrinsic (e.g., chemical composition and structure, hydrophilicity, crosslinking density, water content, elasticity) and extrinsic (e.g., lubricant, normal load, opposing substrate, and sliding velocity) factors affect hydrogel lubrication[13]. Hydrogel friction coefficients can be tailored

[1]Centre for Biomedical Technologies, Queensland University of Technology (QUT), Brisbane, QLD, Australia. [2]Gelomics Pty Ltd., Brisbane, QLD, Australia. [3]Max Planck Queensland Centre (MPQC) for the Materials Science of Extracellular Matrices, Queensland University of Technology (QUT), Brisbane, QLD, Australia. [4]School of Mechanical, Medical and Process Engineering, Faculty of Engineering, Queensland University of Technology (QUT), Brisbane, QLD, Australia. [5]Centre for Genomics and Personalised Health, School of Biomedical Sciences, Queensland University of Technology (QUT), Brisbane, QLD, Australia. [6]Department of Materials, Imperial College London, London, UK. [7]Department of Bioengineering, Imperial College London, London, UK. [8]Institute of Biomedical Engineering, Imperial College London, London, UK. [9]These authors contributed equally: Christoph Meinert, Angus Weekes. e-mail: t2.klein@qut.edu.au

using a variety of chemical and physical alterations to the polymer matrix, including functionalization with boundary lubricant molecules[14,15], or polymer brushes[16], modulation of surface porosity, topography, and charge density[17]. These approaches involve modification of the chemistry or structure of hydrogel bulk or surface properties to achieve low friction surfaces.

The interfacial interaction between water and a substrate is dependent on the hydrophilicity or hydrophobicity of a material, influencing the degree of bound water on the substrate[18–21]. Hydrophilic materials exhibit a greater affinity for water, demonstrating greater bound water than hydrophobic materials, a phenomenon which may affect hydrogel crosslinking, potentially altering mechanical and tribological properties as studied herein[21–23]. Thus, utilization of biomaterials with different hydrophobicity may be used to manipulate hydrogel properties to enhance bioactivity, cyto- and biocompatibility, and ultimately the ability of hydrogel constructs to promote the generation of functional cartilage neo-tissues.

An overarching mechanism to control surface friction of hydrogel constructs without significant alterations to the cellular microenvironment or polymer composition is desirable in cartilage tissue engineering applications. In various studies, Gong et al.[24–26]. have demonstrated that the frictional properties of synthetic vinyl monomer hydrogels, are highly dependent on the hydrophobicity of the substrate on which the hydrogel is crosslinked. Specifically, gels crosslinked on hydrophilic substrates, such as glass or sapphire, exhibit high surface friction, whereas those crosslinked on hydrophobic surfaces, such as polytetrafluoroethylene (PTFE), display highly hydrated, self-lubricating surfaces with low surface friction[24–26], even for the same chemical composition. Here, we sought to investigate whether this substrate-induced effect could be applied to natural hydrogel-based tissue-engineered constructs as an avenue to control their tribological properties without impacting the ability to support neo-tissue formation.

Previously, we have demonstrated that hydrogels composed of gelatin methacryloyl (GelMA) and hyaluronic acid methacrylate (HAMA) support chondrogenic re-differentiation of human articular chondrocytes following expansion in vitro[27,28], enabling generation of mechanoresponsive cartilage neo-tissues with native-like biochemical composition and steadily increasing mechanical properties[9]. However, the frictional properties of hydrogel constructs remain to be optimized to further enhance the clinical relevance of this tissue engineering strategy. Thus, in this work, we demonstrate that photocrosslinking of cell-laden hydrogel precursors in contact with hydrophobic surfaces leads to a significant and long-lasting reduction of surface friction of developing neo-tissue constructs. Hydrogels crosslinked on PTFE display lower crosslinking densities, as well as increased water content and roughness at their surface. These characteristics provide an efficient and durable mechanism for self-lubrication by visco- and poroelastic water exudation under mechanical loading, a biomimetic mechanism similar to native articular cartilage[29], which is retained during neo-tissue development in vitro. We further demonstrate that self-lubricating neo-tissue surfaces limit tissue strain under shear and biaxial mechanical loading, resulting in improvements in mechanically induced extracellular matrix (ECM) formation.

Results and discussion

In the preparation of GelMA/HAMA hydrogels for cartilage tissue culture experiments (Fig. 1A), we first noticed that hydrogel strips crosslinked between PTFE and glass exhibited heterogeneous swelling behavior (Fig. 1B) similar to that reported by Peng et al.[26,30]. This led us to investigate the effect of the substrate upon which a hydrogel is photocrosslinked, on the properties of the hydrogel itself. Handling made differences in surface properties immediately apparent, where PTFE-exposed GelMA/HAMA surfaces appeared more hydrated, lubricious and displayed evidently lower surface friction than hydrogel surfaces exposed to glass (Video SV1, Supplementary Data). These observations were similar to findings previously published by the Gong group using synthetic hydrogels[25,30,31].

Initially we inferred that the observed differences in surface properties may be attributed to the hydrophobicity and hydrophilicity of PTFE and glass crosslinking substrates, respectively[13], confirmed via contact angle analysis (Fig. S1F, Supplementary Data). Further, due to the hydrophilicity of glass, it was inferred that, at the interfacial layer a greater amount of tightly bound water may be present in comparison to hydrophobic PTFE. This hypothesis was assessed via differential scanning calorimetry (DSC), with analyses performed to obtain the thermal profiles of water interfaced with glass or PTFE substrates. The proportion of freezable water (W_f) and non-freezable bound water (W_{nfb}) were calculated, expressed as a percentage of equilibrium water content (EWC) (Fig. S1G–I, Supplementary Data). Statistically significant differences were observed in the water–substrate analyses, with a reduced proportion of tightly bound water present on the hydrophobic PTFE. This provided a potential explanation for the presence of the lubricating surface layer observed in hydrogels crosslinked on PTFE, given the reduced amount of bound water on the hydrophobic substrate, with subsequent tribological tests performed to assess the surface properties of the hydrogels under shear loading. DSC of cell-free bulk hydrogels was also performed, with the results indicating no significant influence of substrate on bulk water composition of gels after swelling (Fig. S1A–E, Supplementary Data).

Tribological tests on cell-free GelMA/HAMA hydrogels confirmed that gel surfaces exposed to PTFE indeed had significantly lower kinetic frictional coefficients μ_{kin} compared to gel surfaces exposed to glass during crosslinking. These ranged between 0.03–0.06 and 0.16–0.25 for PTFE- and glass-exposed gel surfaces, respectively, with μ_{kin} values retained over a period of at least 14 days of incubation in cell culture media in the absence of cells (Fig. S2, Supplementary Data). We next investigated whether this simple effect could be utilized to control the frictional properties of ex vivo engineered cartilage tissues based on human chondrocyte-laden GelMA/HAMA hydrogel constructs (Fig. 2). Our results confirmed that in comparison to glass-exposed construct surfaces, μ_{kin} values of PTFE-exposed construct surfaces were significantly reduced over a range of sliding speeds

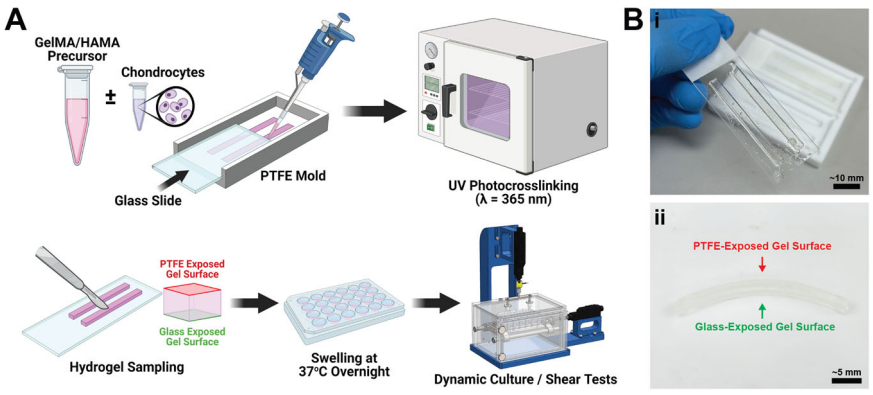

Fig. 1 | GelMA/HAMA hydrogels photocrosslinked between glass and PTFE substrates. **A** Representative method for the preparation of 9.5% w/v GelMA/0.5% w/v HAMA constructs containing 0.05% w/v IC2959, photocrosslinked between glass (green) and PTFE (red) substrates in a mold. **B** Resultant GelMA/HAMA hydrogel strips (i) removed from mold on glass slide, and (ii) after overnight swelling in PBS at 37 °C with gel strip exhibiting curling behavior.

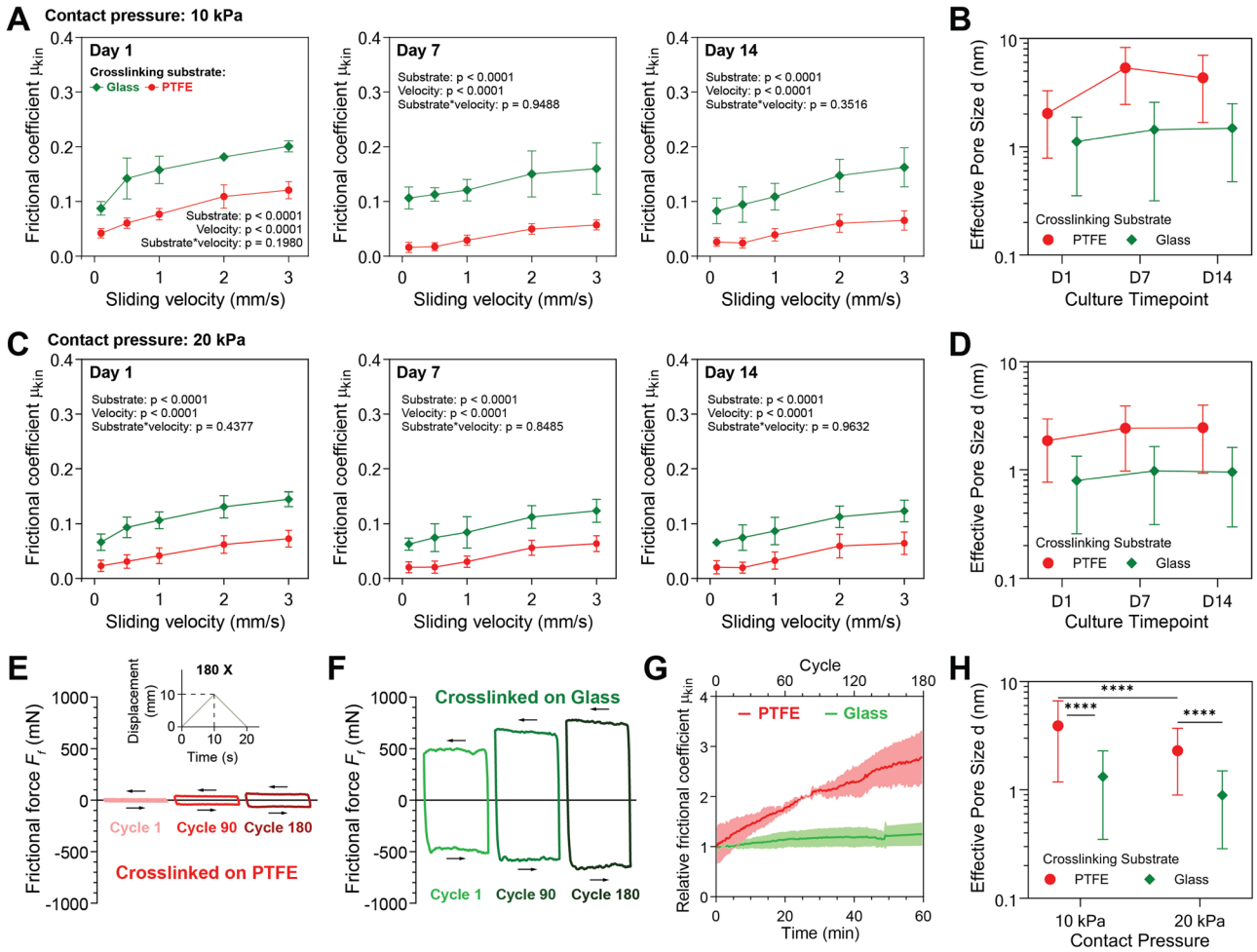

Fig. 2 | Tribological properties of chondrocyte-laden GelMA/HAMA hydrogels photocrosslinked on glass or PTFE substrates. Kinetic friction coefficients of chondrocyte-laden 9.5% w/v GelMA/0.5% w/v HAMA constructs photocrosslinked on glass (green) or PTFE (red) substrates at day 1, 7, and 14 of in vitro culture, with chondrocyte differentiation media used as lubricant, at contact pressures of (**A**) 10 kPa and (**C**) 20 kPa, respectively. Effective hydrodynamic pore size of hydrogel surfaces crosslinked on glass or PTFE at (**B**) 10 kPa and (**D**) 20 kPa, respectively, at day 1, 7, and 14. Representative cyclic frictional responses of GelMA/HAMA hydrogels photocrosslinked on (**E**) PTFE and (**F**) glass substrates, under 10 mm compressive loading after 1, 90 and 180 loading cycles. **G** Relative kinetic friction coefficients μ_{kin} of constructs photocrosslinked on PTFE or glass substrates over loading 180 cycles. **H** Overall effective hydrodynamic pore size of hydrogel surfaces crosslinked on glass or PTFE across the experiment. Values reported as mean ± SD, where symbols indicate significance (****$p < 0.0001$).

(0.1–3 mm s^{-1}) and contact pressures (10 and 20 kPa) (Fig. 2A, C). We also observed lower μ_{kin} in cell-laden gels crosslinked on PTFE as a result of increased culture duration, though only the 10 kPa compression sliding tests of PTFE-exposed gels exhibited statistically significant decreases in μ_{kin} across timepoints, with no statistically significant reductions at 20 kPa compression for either PTFE or glass (Fig. 2A, C and Fig. S3, Supplementary Data). From day 1 to day 14 of culture, PTFE samples subject to 10 kPa compression during sliding, exhibited significant reductions in μ_{kin} of 61%, 71%, 62%, 54% and 53% at sliding velocities of 0.1, 0.5, 1, 2, and 3 mm s^{-1}, respectively; while for glass at 10 kPa, significant reductions were only observed at sliding velocities of 0.5, 1 and 3 mm s^{-1}, namely 34%, 31% and 19%. For samples subject to 20 kPa compression during dynamic culture, slight reductions were observed across sliding velocities, though these were non-significant due to large standard deviations. For samples prepared on glass, only very minimal reductions were observed in the 10 kPa groups from day 1 to day 14 of culture, while negligible differences were observed at 20 kPa compression across timepoints. Thus, the crosslinking substrate may have a long-lasting effect on construct friction, with PTFE showing more promising results in this regard.

According to the biphasic theory for cartilage and hydrogels, interstitial fluid is increasingly exuded from the tissue/gel matrix under continuous loading conditions, leading to a time-dependent increase of μ_{kin} caused by steadily decreasing fluid load support and thus increasing solid-to-solid contact areas[29]. We sought to investigate whether photocrosslinked GelMA/HAMA constructs were able to replicate this physiological behavior and therefore performed reciprocal sliding friction tests for 1 h. These tests revealed that PTFE-exposed gels effectively replicated the viscoelastic and time-dependent frictional behavior previously reported for articular cartilage[29,32], while glass-exposed gels behaved more similar to solids, exhibiting comparatively steady relative μ_{kin} values for 180 cycles (Fig. 2E–G).

The multiphasic structure of tissues and hydrogels leads to a complex interfacial rheological behavior, where gel/tissue-associated macromolecules interact with both the interstitial fluid and the opposing surface. Consequently, traditional models of solid-solid friction and mechanisms of lubrication fail to adequately describe the frictional behavior of hydrogels and tissues which typically display a strong dependency on normal load, sliding velocity, contact area, and other experimental factors[33,34]. As such, several theories have emerged which describe the influence of hydrodynamic (or effective) pore size on the fluid shear frictional properties of hydrogels, specifically at the surface where the interaction of polymer chains and water content dictate lubrication[35]. It must be noted that the hydrodynamic pore size determined herein (Fig. 2B, D, H), may not concur with commonly reported theoretical mesh or pore size calculations, as the hydrodynamic pore size aims to define fluid flow within the porous surface

layer of swollen polymer networks. Thus, the arrangement of extended polymer chains, and concentration of those with free ends near the surface of a hydrogel, are influenced by the crosslinking substrate, as reported herein and indicated within literature, hence influencing frictional behavior[36,37].

In this regard, the hydrodynamic pore size may vary with respect to both shear and normal forces applied, as well as the sliding velocities experienced. At low velocities, the kinetic frictional behavior of μ_{kin} relative to velocity has been reported to provide an estimate of the hydrodynamic pore size in the surface layer as described by Cuccia et al.[35]. This relation may be ascertained using Newton's law of viscosity:

$$F_f = \frac{\eta A v}{d} \quad (1)$$

Where η is the dynamic viscosity of the solvent, A is the surface area, v is the sliding velocity, and d is the hydrodynamic pore size at the hydrogel interface. This conceptual hydrodynamic pore size is variable with respect to the heterogeneous structure of the swollen polymer matrix and is dependent on applied loads[35]. Thus, the hydrodynamic pore sizes at the interfacial hydrogel surface were calculated across timepoints (Fig. 2B, D), with pore size effectively stable throughout the 14-day culture period. Notably, significant differences were observed between the hydrodynamic pore size of constructs crosslinked on glass compared to PTFE overall (Fig. 2H), with the mean data indicating significantly smaller hydrodynamic pores within glass-exposed hydrogels. Further, a decrease in size in both groups was observed with increased contact pressure (Fig. 2H).

Based on the relation between effective pore size and μ_{kin}, the interaction of near-surface polymer chains with a substrate may contribute to the frictional properties under applied loading. In turn, this may dictate the interfacial capacity for dynamic water release and retention[35,38,39]. Kim and Dunn[38,39] describe a potential mechanism for the maintenance of interfacial hydration under loading, whereby an increased presence and alignment of well-solvated polymer chains with free ends in the near-surface layer will retain water more than those with less free polymer chains, hence contributing to frictional performance[36]. Further, the friction coefficient dependence on crosslinking substrate hydrophobicity is outlined[37], emphasizing the influence of adjacent substrate on polymer chain arrangement[35]. Hence, for hydrophobic materials, specific interactions between free hydrogel polymer chains and the crosslinking substrate that contribute to friction, would be limited, leading to improved frictional performance, as characterized herein, and coincident with our hypotheses associated with bound water content of crosslinking substrates.

Following the functional characterization of the substrate-induced effect on hydrogel and cartilage neo-tissue construct surface friction, we performed several studies to investigate the underlying mechanism governing this phenomenon. Our initial observation of anisotropic swelling behavior leading to curved hydrogel strips (Fig. 1B) in which the glass-exposed surfaces were always facing the center of curvature, indicated that PTFE-exposed surfaces had a higher swelling capacity, and therefore local water content, compared to glass-exposed surfaces. A higher swelling capacity with an otherwise unchanged biochemical gel composition in turn suggested lower macromer crosslinking densities at PTFE-exposed gel surfaces. We therefore performed topographical, mechanical, and biochemical studies of gel constructs using atomic force microscopy (AFM) and developed a method to visualize the presence of unreacted methacryloyl groups (Fig. 3).

Collectively, these investigations suggested the presence of loosely crosslinked, highly hydrated dangling polymer chains at PTFE-exposed gel surfaces. The AFM analyses (Fig. 3A) of the PTFE-exposed construct surfaces displayed significantly higher arithmetical mean (Fig. 3B) and root mean squared (RMS) roughness (Fig. 3C) compared to glass-exposed gel surfaces, suggesting that the increased profile depth may contribute to reducing PTFE-exposed construct friction by acting as nano-scale reservoirs for lubricating fluid which is exuded during sliding motion. Furthermore, we found that PTFE-exposed surfaces had significantly lower compressive moduli (Fig. 3D), consistent with decreased crosslinking densities compared to glass-exposed surfaces. Lastly, we used a fluorescent monomer capable of reacting with uncrosslinked methacryloyl groups in GelMA and HAMA, fluorescein-o-methacrylate, to spatially map the location of unreacted methacryloyl groups in gel construct sections (Fig. 3E). This analysis revealed the presence of unreacted methacryloyl groups at the PTFE-exposed construct surface, as well as along the edges which were also exposed to PTFE within the molds. Uncrosslinked groups peaked at 125 μm and were detected up to approximately 250 μm from the construct surface, demonstrating that the substrate-induced partial inhibition of monomer polymerization spatially reached beyond the immediate gel/substrate interface.

One limitation of this study was that the influence of hydrogel thickness on crosslinking efficacy or tribology was not studied. Based on our findings from surface topography and crosslinking density (Fig. 3E), we do not anticipate significant effects of hydrogel thickness on tribological properties, given the microscopy images of unreacted methacryloyl groups indicate consistent crosslinking throughout the bulk of the hydrogel, with unreacted groups observed only at the edges exposed to PTFE. Thickness-related concerns would become more relevant for very thick samples, where limited penetration of visible light crosslinking might occur. Ultimately, future work will be necessary to investigate the role of hydrogel thickness in this regard.

While the molds used represent a fully enclosed system, with the substrate-induced effect the primary mechanism being studied here, differences in oxygen diffusivity between glass and PTFE substrates may have contributed to the observed local effects on hydrogel crosslinking and mechanical/tribological properties. Work by Spencer, et al., clearly demonstrates that oxygen available from the substrate inhibits crosslinking near the surface for several hydrogel-substrate systems, resulting in differences in compressive modulus and friction coefficient[40,41]. Future studies with controlled oxygen availability from the substrates are warranted to determine if these crosslinking conditions have long-term effects on chondrocyte differentiation and ECM production. Further, a similar approach could be used to induce an oxygen gradient to mimic the in vivo hypoxic environment of cartilage through careful design of the culture vessel. Ultimately, if localized oxygen control could be achieved by altering the substrates upon which a hydrogel is prepared and cultured, tuneable internal environments could be induced without the use of oxygen-scavenging or oxygen-releasing microparticles such as those described in literature[42,43].

Furthermore, given this study investigates only two materials as crosslinking substrates, namely PTFE and glass, future work may benefit from incorporating alternative materials and combinations of these to determine effects on tribology. While different materials would be expected to influence surface crosslinking and tribology, additional testing would be necessary to determine if the combination of substrates affect each other and the resultant hydrogel properties. Thus, experimental planning would need to consider the application of such studies given the extensive number of potential materials and combinations.

The mechanical environment of articular cartilage is an important regulator of chondrocyte function and tissue homeostasis. Moderate mechanical stress induces anabolic processes and contributes to cartilage ECM maintenance and remodeling. Excessive stress, on the other hand, is a major risk factor for the development of degenerative diseases such as osteoarthritis. Tissue shear strain in response to biaxial loading and consequently strain experienced by chondrocytes is linearly proportional to the product of μ and the contact pressure[44], providing a direct causative link between the frictional properties of articular cartilage and the health of the tissue. In healthy diarthrodial joints, nearly frictionless articulation of opposing cartilage surfaces effectively reduces shear strains in the tissue to maintain cartilage homeostasis and promote ECM production and turnover[45,46].

Acute injury, changes in biomechanics, or inflammatory events, however, result in a reduced lubricating function and increased frictional

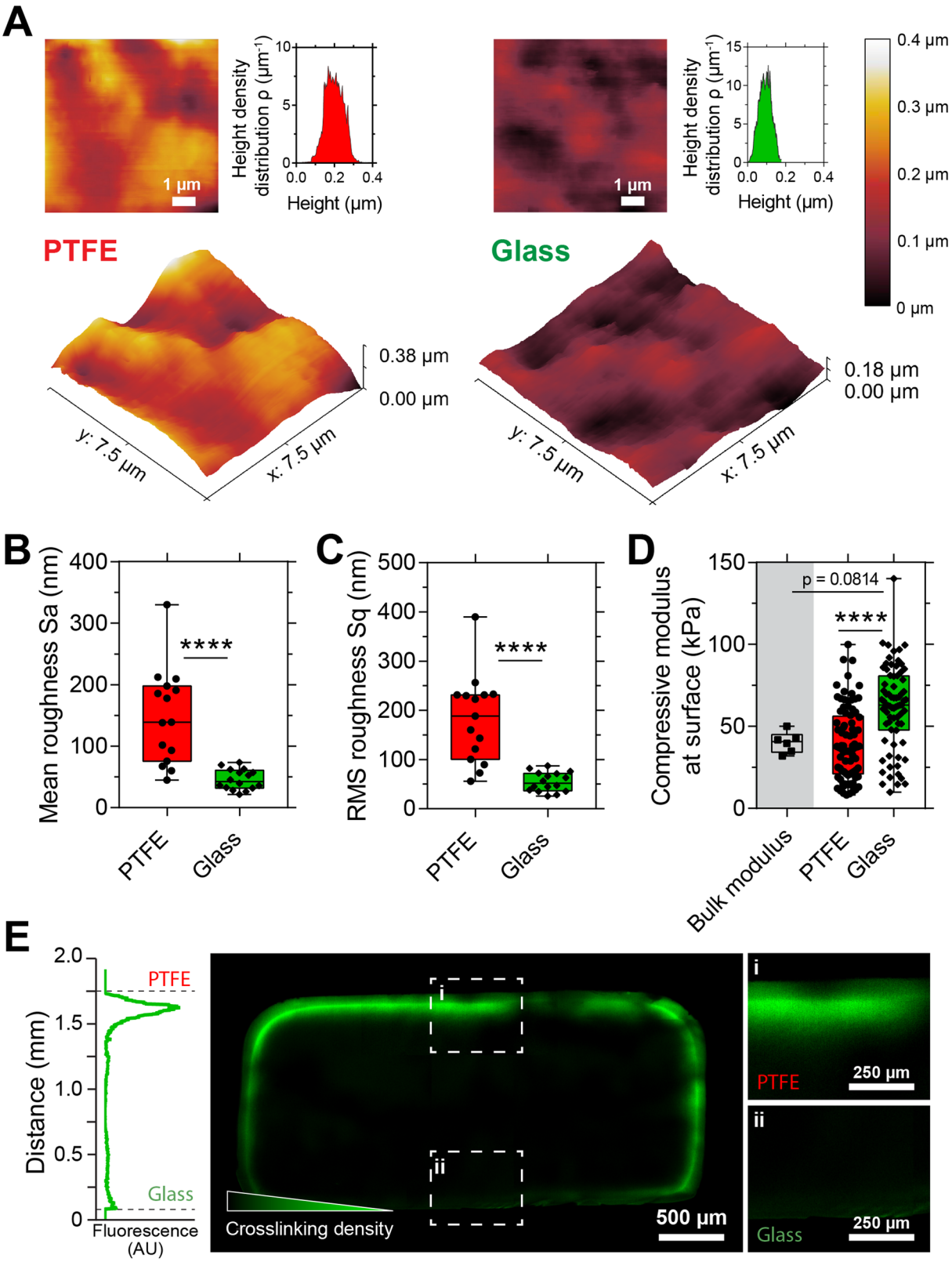

Fig. 3 | Characterization of surface topography, surface mechanics and cross-linking density of GelMA/HAMA hydrogels crosslinked on glass and PTFE substrates. Topographical analyses enabled via AFM to obtain **A** surface roughness profiles of glass- and PTFE-exposed hydrogels, corresponding to the **B** arithmetical mean, and **C** root mean squared (RMS) roughness, as well as the **D** compressive surface modulus of respective hydrogels at the surface in comparison to the bulk modulus obtained via whole construct compression testing. **E** Fluorescence intensity profile and representative fluorescence images of hydrogels crosslinked between glass and PTFE, visualized with fluorescein-o-methacrylate for spatial analysis of unreacted methacryloyl groups in hydrogel sections (10 µm sections). Box-plots presented with median center line and all points shown, with upper and lower quartiles presented and whiskers extending from minimum to maximum, where symbols indicate significance (****$p < 0.0001$).

forces between cartilage surfaces[47–50]. As a result, peak tissue shear strains during joint articulation are significantly increased and cause excessive mechanical stresses which shift cellular homeostasis towards catabolic processes and the progressive deterioration of the tissue[51], eventually resulting in the development of osteoarthritis[44]. However, despite its importance for the maintenance of native cartilage, characterization of the functional relationship between the frictional properties of tissue-engineered cartilage and chondrocyte behavior upon mechanical stimulation is limited[9,52].

This prompted us to investigate whether the crosslinking substrate-induced effect on surface frictional properties influenced cellular behavior and the properties of tissue-engineered cartilage under loading conditions. First, we assessed the magnitude of shear strain (E_{xz}) in tissue-engineered cartilage constructs under sliding shear motion mimicking physiological joint articulation (Fig. 4A–C). We embedded fluorescent microspheres in low and high friction GelMA/HAMA constructs prepared by photocrosslinking on either PTFE or glass, respectively, compressed the constructs to ~10% strain, and applied sliding shear motion (1 mm amplitude, 1 mm s^{-1}) using a custom microscope-mounted loading device. Digital image correlation (DIC) was used to track particle displacement and calculate local E_{xz} throughout the cross-sectional area of the constructs. This analysis corroborated our previous work[17] and demonstrated that the magnitude of E_{xz} was highly dependent on the surface frictional properties of GelMA/HAMA gels. Similar to healthy native cartilage, low-friction constructs crosslinked on PTFE displayed minimal E_{xz} throughout the depth of the construct (~0.1–1.5%), while constructs crosslinked on glass, on the other hand, underwent substantially higher magnitudes of E_{xz} (~0.1–4.5%) under the same loading conditions (Fig. 4C). We then proceeded to investigate whether differences in surface friction and the resulting effects on construct E_{xz} may regulate neocartilage formation under biomimetic loading conditions.

Human articular chondrocytes from adult donors were expanded to passage 1 and encapsulated in GelMA/HAMA gels. Following 14 days of static preculture to facilitate the formation of a pericellular matrix, constructs were exposed to intermittent biaxial loading for an additional 14 days using a custom mechanical stimulation bioreactor system (Fig. 4A, B) developed by us previously[9]. Live/dead analysis demonstrated high cell viabilities in all loaded and static conditions, independent of the crosslinking substrate (Fig. 4D, E). There were also no significant effects on the physical properties of neocartilage constructs which increases in wet weight (Fig. 4F) and compressive moduli (Fig. 4G) to a similar extent in all experimental groups and loading conditions, with DNA content (Fig. 4H) also similar at day 28 across groups. Relative GAG/DNA content within cartilage neotissues, however, was highly dependent on the surface frictional properties of the construct, with the relative accumulation of GAGs significantly greater in PTFE-exposed exposed low-friction constructs (Fig. 4I).

While this study focused primarily on shear and frictional testing to assess surface-related kinematics, cyclic compression was included in the dynamic culture studies to mimic physiological loading patterns experienced in vivo. While our hydrogel materials possess compressive moduli in the low physiological range of native cartilage, these hydrogels exhibit advantageous frictional properties which may be particularly relevant in the ongoing development of in vitro cartilage models and cartilage repair therapies.

To improve the compressive performance and failure properties of these low-friction hydrogels, application or combination of these manufacturing methods with alternative materials may achieve low-friction hydrogels while maintaining the beneficial frictional kinematics observed here. Specifically, these low-friction manufacturing methods may be combined with our previously published work where the addition of glycol chitosan to GelMA increased the compressive modulus and adhesive crosslinking properties significantly, while maintaining high cell viability[53,54]. In small defects, the hydrogel alone may be suitable to handle the loading that is shared with the surrounding cartilage as we have shown in vitro. However, for larger defects, where the gel is bearing the load independent to surrounding tissue, failure may occur. Thus, we have developed fibre-reinforcement techniques using melt electrowritten (MEW) scaffolds, increasing the load-bearing capacity of our constructs substantially, replicating cartilage-like mechanical properties and robustness[11,55,56]. Thus, as previously noted, future work is required to ascertain the degree to which tribological properties of other hydrogel systems may be influenced by crosslinking substrate hydrophobicity. However, translation of the methods reported here, we anticipate similar effects on surface friction to be achievable in other hydrogel systems, particularly our GelMA-based hydrogel systems.

Subsequent immunofluorescence imaging and analysis (Fig. 5) indicated mechanical stimulation of PTFE-crosslinked, low-friction neocartilage significantly enhanced the biosynthesis and accumulation of ECM, resembling healthy hyaline cartilage, while stimulation of glass-crosslinked, high friction constructs resulted in phenotypes linked to chondrocyte dedifferentiation and cartilage disease. Key biochemical features of native articular cartilage include the abundant presence of collagen type II and proteoglycans such as aggrecan which interact with a fluid environment to provide the tissue with its unique biomechanical properties. The expression of these markers is thus commonly used to assess tissue formation in engineered constructs. Intermittent biaxial mechanical loading had a stimulatory effect on the accumulation of collagen type II, the main structural protein of healthy hyaline cartilage, with fluorescence intensity significantly more pronounced in low friction constructs (~3.5-fold increase) than high friction constructs (~2.2-fold increase) relative to static cultured hydrogels (Fig. 5A).

Immunoreactivity for collagen type I, a marker of chondrocyte dedifferentiation and mechanically inferior fibrocartilage, was minor in both static controls and mechanically stimulated low-friction neocartilage constructs, but significantly higher in loaded high-friction constructs (~1.7-fold increase compared to static controls) (Fig. 5B). We also found that the expression of accumulated aggrecan (Fig. 5C) was significantly reduced in loaded high-friction cartilage constructs (~0.5-fold increase compared to static controls). Collectively, these data demonstrate that the surface frictional properties of neocartilage constructs, similar to native tissues, are a crucial regulator of E_{xz} and consequently cellular metabolism in biomimetic loading conditions. Importantly, photocrosslinking on PTFE surfaces had no measurable detrimental effects on chondrocyte viability and function, and significantly improved cellular response to loading, based on immunostained expression of essential ECM components.

Given the high relative stiffness of the GelMA/HAMA hydrogels within which the human articular chondrocytes were encapsulated herein, spheroid formation, rather than a branched ECM network, was expected across the 28-day study, coinciding with cellular proliferation under mechanical stimulation. This spheroid formation was observed via fluorescence microscopy analyses of samples stained for both cellular viability (Fig. 4D) and collagen components (Fig. 5D). These results align with our previously published studies in the 3D cell culture of cartilage neo-tissues, whereby chondrocyte spheroid formation in both natural[17,53] and synthetic[57] hydrogels was observed with negligible branching despite the production and accumulation of essential collagen components of the cartilage ECM.

Gene expression analyses were also performed following the final loading cycles, yet no significant differences were observed between loaded constructs crosslinked on glass or PTFE (Fig. S4, Supplementary Data). Similar to our previous studies[9], cell-laden hydrogels cultured under dynamic loading exhibited increased *COL2A1* and *PRG4*, as well as decreased *COL10A1*, relative to static cultured constructs, with this noted in both PTFE and glass groups. For *ACAN*, *COL1A1*, *MMP2* and *MMP13*, no statistical differences were observed, with stable expression irrespective of loading or crosslinking substrate.

While the 28-day dynamic in vitro cell culture study reported herein has provided promising results, cartilage repair is a particularly slow process[58]. Thus, long-term studies with additional timepoints would be valuable for assessing the stability and durability of our low-friction hydrogels under prolonged mechanical loading. Thus, in the planning of

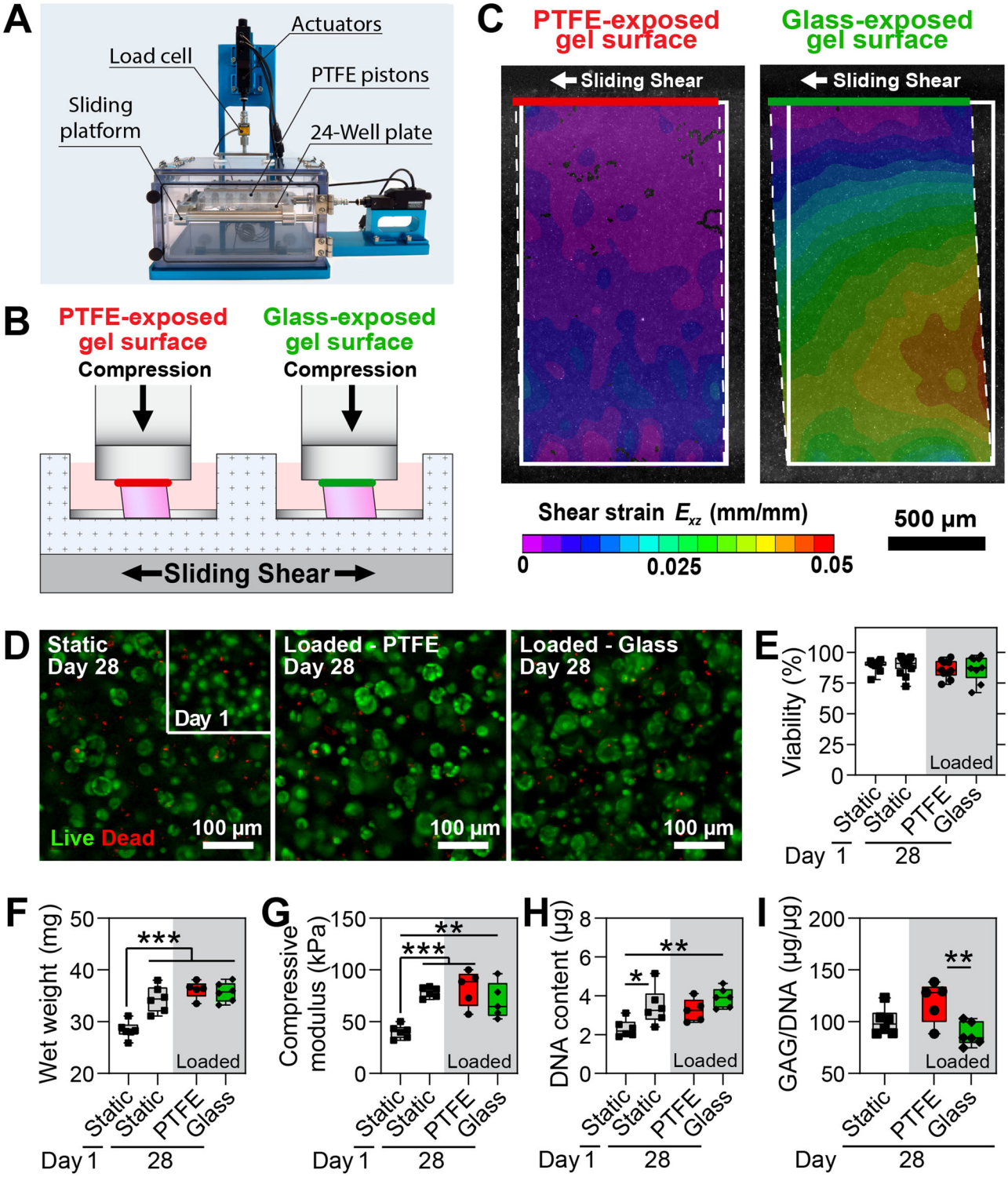

Fig. 4 | Biochemical assessment of static and dynamic cultured chondrocyte-laden GelMA/HAMA hydrogels crosslinked on glass and PTFE substrates, after 28 days of cell culture. **A** Schematic of mechanical stimulation bioreactor for the application of (**B**) biaxial shear and compressive loading to hydrogel constructs in vitro. **C** Digital image correlation (DIC) analysis of the cross-sectional area of hydrogels depicting differences in shear strain (E_{xz}). **D** Representative images and **E** quantification of cell viability within free-swelling and intermittently loaded hydrogels after 28 days, with live (green) and dead (red) stained chondrocytes imaged via fluorescence microscopy; cell viability expressed as percentage of live to total cells. Biochemical assessment of cultured hydrogels indicating **F** construct wet weight, **G** compressive moduli, **H** DNA content, and **I** GAG/DNA content at 28 for comparison of free-swelling and loaded hydrogels crosslinked on glass and PTFE substrates. Box-plots presented with median center line and all points shown, with upper and lower quartiles presented and whiskers extending from minimum to maximum, where symbols indicate significance (****$p < 0.0001$, ***$p < 0.001$, **$p < 0.01$, *$p < 0.05$).

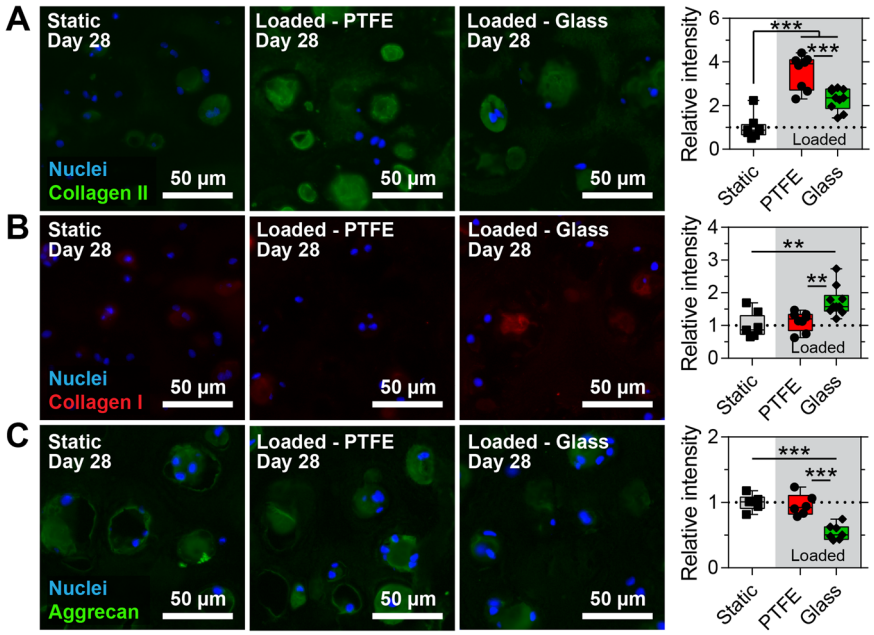

Fig. 5 | Immunofluorescence imaging of static and dynamic cultured chondrocyte-laden GelMA/HAMA hydrogels crosslinked on glass and PTFE substrates, after 28 days in vitro. Representative images and corresponding quantification of relative fluorescent intensity of **A** collagen II, **B** collagen I, and **C** aggrecan, within static and intermittently loaded hydrogels after 28 days in vitro culture. Boxplots presented with median center line and all points shown, with upper and lower quartiles presented and whiskers extending from minimum to maximum, where symbols indicate significance (***$p < 0.001$, **$p < 0.01$).

future experimental work, long-term follow-up studies are required to evaluate the performance of these low-friction hydrogels over extended periods, which may result in enhanced ECM accumulation thus providing determination of specific differences in gene expression results. While gene expression differences were not significant at 28 days under loading, extensive ECM accumulation was evident in PTFE-crosslinked constructs, as indicated by strong interterritorial and pericellular staining for collagen II. This suggests that protein-level changes and matrix deposition occurred, but gene expression may have stabilized by this stage, reflecting a more mature chondrocyte phenotype rather than an ongoing transcriptional response.

Importantly, transcriptional activity does not always directly correlate with protein production, as gene expression represents an early regulatory step, while post-transcriptional modifications, translation efficiency, and protein turnover influence final ECM deposition[59–61]. Previous studies have shown that cartilage ECM accumulation can be heavily regulated at the post-translational level, with enzymatic processing and matrix incorporation occurring independently of steady-state mRNA levels[62,63].

Additionally, with appropriate data and resources, there exists potential for future preclinical animal studies for extended performance assessment in vivo. Both extended in vitro and potential in vivo work would further develop our understanding of construct longevity, cellular behavior long-term, and maintenance of tribological properties, to ascertain suitability for clinical translation. Additionally, we acknowledge that increasing the sample size, donor number, and number of constructs would enhance the robustness and reproducibility of our findings. Future work will incorporate larger sample sizes to further investigate the limitations associated with the gene expression results and strengthen the translational potential of our findings pertaining to hydrogels with tuneable tribological properties.

For clinical applications of tissue-engineered cartilage constructs, matrix-assisted chondrocyte implantation (MACI) represents the procedure by which autologous chondrocytes, derived from a tissue biopsy, are isolated and expanded in vitro, embedded in a hydrogel or seeded onto a 3D scaffold, and implanted into a cartilage defect to promote tissue regeneration[64]. A variety of hydrogels such as fibrin/hyaluronic acid[65,66], polyglactin/polydiaxanone[67,68], and collagen-based constructs[69–71] have been investigated as cell carriers in clinical trials. While most of those studies demonstrated safety and feasibility in stage I and II trials, randomized studies revealed largely unsatisfactory outcomes that were similar to microfracture surgery, a simpler and less expensive one-step bone marrow stimulation procedure facilitating the growth of fibrocartilage repair tissue[64,71,72]. This led to the termination or withdrawal of most MACI products except for a few which remain available in select countries. Increasing evidence suggests that injectable hydrogels may provide a more suitable cellular microenvironment for hyaline cartilage regeneration, with several products based on cell-laden or cell-free hydrogels having been investigated in clinical trials[73–75]. Similarly, our low-friction GelMA/HAMA chondrocyte-laden cartilage neo-tissues may be implanted via such methods in future preclinical and clinical applications.

Surgical procedures are carried out by arthroscopy or arthrotomy and involve injection and in situ polymerization of the gel biomaterial, in some cases, using photopolymerization[64]. To simulate associated workflows and demonstrate the clinical relevance of our findings, we prototyped a handheld UV-A curing device incorporating a flexible PTFE membrane mounted on a tripod to cover cartilage defects during in situ photopolymerization (Fig. 6). First, a full thickness chondral defect of 8 mm diameter was created in the medial femoral condyle of a bovine stifle joint ex vivo. Then, the curing device was placed over the defect, ensuring the PTFE membrane covered and sealed the entire lesion. A GelMA/HAMA hydrogel precursor solution containing blue food dye for visualization was injected through a PTFE membrane into the defect using a syringe and needle and subsequently polymerized using 365 nm UV light exposure for 15 s. Visual and physical examination confirmed that the polymerized hydrogel entirely filled the lesion and conformed to the lesion size, shape, and depth, demonstrating a potential clinical workflow. In combination with the mechanical, tribological and in vitro data obtained within this study, these results support the hypotheses proposed, for the development of hydrogel constructs with improved surface friction properties, suitable for use as regenerative treatments in osteochondral defect repair.

While this ex vivo study clearly demonstrates the potential for clinical application of our low-friction hydrogel system, the properties of the hydrogels injected and crosslinked in situ were not specifically assessed. Primarily, this was a physical limitation whereby the crosslinked materials could not be removed from the joint defect without damaging the integrity of the implant. While we do not anticipate significant differences in frictional performance given the consistent material properties of PTFE, it must be considered that the surface properties of these gels crosslinked through the PTFE membrane and in contact with native tissue may exhibit slight variations to our in vitro models. Replication and extension of the experiments performed herein would be required to assess this directly in future work, with this to be potentially assessed in future animal studies.

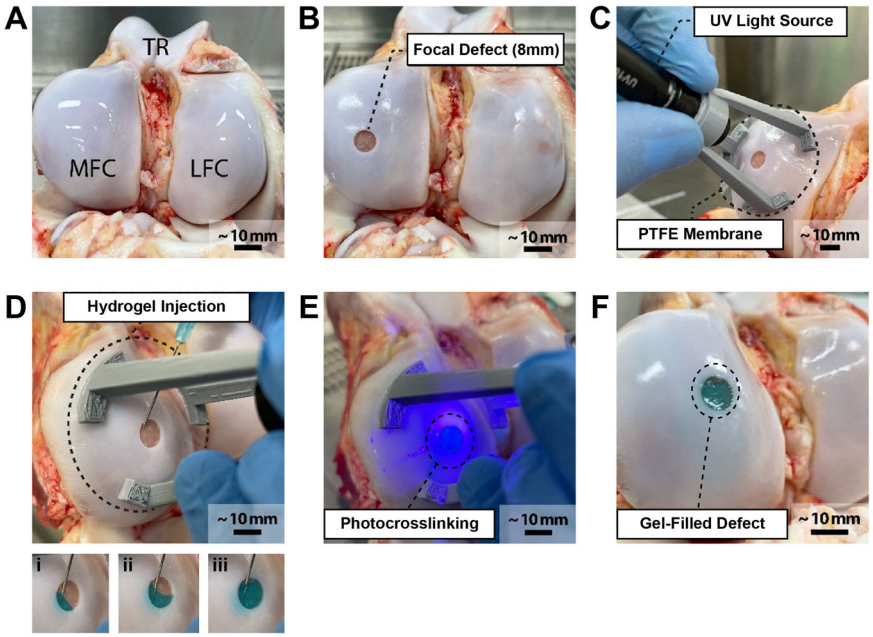

Fig. 6 | Simulated clinical workflow for implantation of GelMA/HAMA hydrogels in a full thickness cartilage defect. Representative stages of hydrogel injection: **A** bovine stifle joint, **B** creation of full thickness chondral defect (8 mm diameter) in the medial femoral condyle, **C** custom handheld UV-A curing device with flexible PTFE membrane through which precursor may be injected, **D** injection of GelMA/HAMA precursor (stained blue for visualization) using a syringe and needle where (i–iii) indicate progressive filling of defect through transparent PTFE film, **E** in situ photopolymerization of the **F** GelMA/HAMA hydrogel using 365 nm UV light exposure for 15 s.

Throughout this study, the photoinitiator used for photocrosslinking of methacrylated hydrogels was IC2959; which, despite its proven cytocompatibility and extensive use in cartilage tissue engineering[55,76,77], possesses some limitations. Namely, given the molar extinction coefficient of IC2959 at 365 nm, the wavelength typically used for hydrogel photopolymerization, is very low and trails off almost entirely before 370 nm[78], hydrogel crosslinking efficiency is quite limited. Further, UV irradiation of hydrogels may lead to the formation of reactive oxygen species and subsequent cell damage[79]. More recently, visible-light photoinitiators such as lithium phenyl-2,4,6-trimethylbenzoylphosphinate (LAP) have been increasingly applied for photopolymerization of cell-laden hydrogels with very good cytocompatibility and short gelation times[80,81]. As such, exploring visible-light photoinitiators, such as LAP, could indeed enhance the safety and clinical relevance of our approach. Future work would therefore be required to characterize the tribological properties of photocrosslinked hydrogels prepared with alternate systems.

However, we hypothesize that differences in frictional properties will be negligible with respect to photoinitiator used. This is based on the inference that the primary mechanism by which hydrogel surface friction is reduced herein is predominantly substrate related, as originally described by Gong et al.[24,25]. In conjunction with existing literature surrounding this phenomenon in synthetic polymer materials, the results of our study aim to develop our general understanding of this mechanism, while presenting a clinical application of this using our natural hydrogel material and in situ photocrosslinking. Further, our study aimed to delve deeper into the mechanisms by which substate-induced material properties at both the surface and overall, are influenced. We believe this study represents a significant contribution to the field which may inform the biofabrication of tissue-engineered hydrogel constructs for clinical applications, with potential for further work in future.

Thus, future work may be suitable to investigate the observed phenomena in various alternative hydrogel systems. To test these hypotheses, manufacture of hydrogel constructs with reproducible bulk mechanical properties, manufactured with alternative photoinitiators is required, with replication of the mechanical tests performed to directly compare performance. While minimal differences in tribological properties would be expected, modification of our system to improve safety and efficacy would be beneficial in the context of clinical translation.

While this study solely investigates GelMA/HAMA hydrogels and their use in cartilage neo-tissue generation, the underlying principles associated with the observed tribological effects on hydrogel mechanics and chondrocyte behavior are likely to extend to other hydrogel systems, both natural and synthetic, albeit at different degrees of influence. Alternative hydrogel systems which may be investigated in our future work, to assess crosslinking substrate induced effects on tribology, include GelMA, GelMA/alginate, GelMA/chitosan, as well as collagen, or synthetic polymer-based systems such as PEG and PVA materials, of which each possess advantageous properties for cartilage tissue engineering. Gong et al.[24,25,30], have investigated a range of synthetic hydrogel systems crosslinked on various substrates, with these hydrogels crosslinked via radical polymerization.

We hypothesize that if surface tribology can be improved in various natural hydrogel systems, similar effects such as the promotion of chondrocyte differentiation and ECM production may be observed in vitro. To compare such systems to the results reported herein, future studies would require matched mechanical conditioning and testing protocols, while consideration must be given to the degree of crosslinking, hydrogel stiffness, and the ability to modulate oxygen availability within these distinct systems. These studies would provide better understanding of the general applicability of the observed results, and allow us to identify key factors that govern cellular behavior in response to loading across a broader range of hydrogel systems.

Ultimately, future application of this work may enable the biofabrication of hydrogel constructs with tuneable frictional properties, dependent on the substrate interface. Further, specific frictional properties may be combined with other mechanisms, including those previously developed by us, where to match key mechanical characteristics of cartilage, we have developed methods to reinforce intrinsically soft hydrogels using highly ordered melt-electrowritten polycaprolactone microfiber scaffolds[11,55,56]. This biofabrication strategy enabled us to tailor key mechanical properties such as the compressive and equilibrium moduli, Poisson's ratio, as well as viscoelastic characteristics, including the storage and loss modulus, to match the properties of human cartilage[11], while retaining large volumetric fractions of the cell-instructive hydrogel matrix for cell encapsulation and neotissue formation. The concept has been further developed to the extent that we can now generate depth-dependent mechanical properties mimicking the zonal nature of articular cartilage[82]. Thus, future studies into the development of reinforced hydrogel constructs with specific frictional properties, based on inclusion of the findings of our work herein, may lead to potential improvement of mechanobiological properties in cartilage tissue engineering.

Conclusion

The results of our study demonstrate that the surface frictional properties of hydrogel-based engineered cartilage tissues can be efficiently minimized using photopolymerization on PTFE substrates. We show that the hydrophobic nature of PTFE partially inhibits crosslinking at the construct surface, to result in loosely crosslinked polymer chains, providing efficient and durable self-lubrication by viscoelastic water exudation under mechanical loading. Importantly, this mechanism reduces tissue shear strains in physiological loading conditions while maintaining the favorable mechano-responsive microenvironment of GelMA/HAMA hydrogel constructs. Within these systems, chondrocytes maintained high viability and matrix deposition when subject to long-term intermittent mechanical stimulation in vitro. Thus, the substrate-induced frictional effect has been characterized for our natural hydrogel-based tissue-engineered constructs, with this representing an avenue to control tribological properties without impacting neo-tissue formation. Incorporation of these findings toward the development of hydrogels with tuneable tribological properties, is expected to further progress the biofabrication of tissue-engineered cartilage.

Methods

Macromer synthesis

Gelatin methacryloyl (GelMA) and hyaluronic acid methacrylate (HAMA) were synthesized as previously published[27,83–85]. In brief, porcine skin gelatin (type A, 300 bloom; Sigma Aldrich, St. Louis, MO, USA) was dissolved in phosphate-buffered saline (PBS, pH 7.4; Invitrogen, Carlsbad, CA, USA) at 10% w/v and reacted with 0.6 g of methacrylic anhydride (MAAh) per gram of gelatin for 1 h at 50 °C under constant stirring. Hyaluronic acid (HA, molecular weight 0.86 MDa, Novozymes, Denmark) was dissolved in PBS at 1% w/v and reacted with a 5-fold molar excess of MAAh over HA hydroxyl groups for 24 h on ice at pH 8. Insoluble MAAh and low molecular weight by-products were removed by dialysis against ultrapure water (MilliQ, Merck Millipore) and the pH of the dialysed products was adjusted to 7.4, after which macromer solutions were lyophilized and stored at −20 °C until use.

Hydrogel preparation

9.5% w/v GelMA and 0.5% w/v HAMA were dissolved in PBS containing 0.05% w/v Irgacure 2959 (1- [4-(2-hydroxyethoxy)-phenyl]-2-hydroxy-2-methyl-1-propanone; BASF, Ludwigshafen, RLP, Germany) at 37 °C. Hydrogel precursor solutions were transferred into a custom polytetrafluoroethylene (PTFE) casting mold and covered with a laboratory glass slide, followed by exposure to 365 nm light at an intensity of ~2.6 mW cm^{-2} in a CL-1000 crosslinker (UVP, Upland, CA, USA) for 15 min, to produce constructs with dimensions of 4 mm × 4 mm × 2 mm (L × W × H). Hydrogels were removed from the casting mold and allowed to swell in PBS or Gibco™ high-D-glucose DMEM (Dulbecco's Modified Eagle Medium, ThermoFisher Scientific, QLD, Australia) 37 °C overnight before further use.

Frictional testing

Measurement of hydrogel surface friction was performed using a custom reciprocating tribometer that enables control of normal force (F_N) and lubricant temperature. The tribometer was attached to an Instron 5848 microtester configured horizontally with a 5 N load cell (Instron, Melbourne, VIC, Australia). Hydrogels were fixed to the apparatus with epoxy adhesive (Loctite, Henkel, Duesseldorf, Germany) without compromising the gel surface. Defined normal forces of 160 mN, and 320 mN were applied onto the hydrogel constructs resulting in contact pressures of 10 kPa and 20 kPa, respectively. Frictional forces were assessed against PTFE (same material as the loading pistons in the mechanical stimulation bioreactor) over a sliding distance of 10 mm for 5 reciprocating cycles at constant sliding velocities ranging from 0.1 to 3 mm s^{-1} in high-D-glucose basal chondrocyte medium with ITS-G (100 × dilution) and 1.25 mg mL^{-1} bovine serum albumin (BSA). Determination of these low sliding speeds was intended to provide data regarding the tribological properties of the hydrogels while maintaining the system within a mixed or boundary lubrication regime, in line with the work of Katta et al.[86], as described in their early study of cartilage frictional properties. For long-term frictional tests, a normal force of 320 mN (20 kPa contact pressure) and a sliding velocity of 1 mm s^{-1} was applied. Kinetic frictional coefficients μ_{kin} were calculated for each sample based on the average measured frictional forces (F_f) and the applied F_N, where:

$$\mu_{kin} = \frac{F_f}{F_N} \tag{2}$$

The long-term reciprocal sliding friction tests, performed on cell-free constructs to ascertain frictional kinematics prior to dynamic cell culture studies, were performed for 1 h to match the daily dynamic loading duration implemented in dynamic culture, as applied in our previous dynamic culture studies[9]. This established cyclic compression protocol was determined to provide controlled, reproducible and stable mechanical stimulation for dynamic culture of hydrogel constructs in our bioreactor system.

Atomic force microscopy (AFM)

AFM measurements were performed using a Keysight Technologies 5500 AFM (Keysight Technologies, CA, USA) with a Nanoworld PNP-DB cantilever (Nanoworld, Neuchâtel, Switzerland) with a spring constant of 0.05 N m^{-1}. Topographical scans were performed in contact mode at 3 ROIs across the sample, and the resulting data was processed using Gwyddion software. Force volume spectroscopy was performed across 3 ROIs on the sample, and the resulting data was analyzed by applying the Hertz model to the force curves using the AtomicJ software.

Characterization of hydrogel crosslinking density

To spatially characterize the presence of unreacted methacryloyl groups in hydrogels crosslinked between glass and PTFE substrates, fluorescein-o-methacrylate (568864; Sigma Aldrich, St. Louis, MO, USA), a fluorescent monomer with an excitation spectra at 490 nm, which is capable of reacting with uncrosslinked methacryloyl groups, was used. GelMA/HAMA hydrogels were prepared as previously described, with the inclusion of 1% w/v fluorescein-o-methacrylate, photocrosslinked within a PTFE mold covered with a glass slide, then incubated overnight in PBS. Gels were sectioned (10 µm sections) and prepared for imaging using a Zeiss Axio epifluorescence microscope (Zeiss Axio Imager 2). Fluorescence images were obtained to visualize uncrosslinked methacryol groups within the GelMA/HAMA hydrogels, with fluorescence intensity profiles across the gel sections obtained for spatial analysis.

Assessment of hydrogel shear deformation

GelMA/HAMA hydrogel precursor solutions were prepared as described above. Cell-free hydrogels containing Fluoresbrite® fluorescent microspheres (Polysciences, Taipei, Taiwan; 10 million microspheres per mL) were prepared and photocrosslinked as described, and incubated overnight in PBS. A custom microscope-mounted mechanical loading system capable of applying precise shear stimulation mimicking physiological joint articulation, was employed for the application of sliding shear motion to the hydrogels, with lower gel surface movement restricted. Gels were compressed to ~10% strain to stabilize samples for frictional imaging without altering bulk morphology and subjected to 1 mm amplitude sliding shear motion at 1 mm s^{-1}, mimicking dynamic cell culture shear and physiological loading. Digital image correlation (DIC) software (Vic-2D DIC; Correlated Solutions, Columbia, SC, USA) was used to track particle displacement within sequential microscope images obtained for calculation of the local E_{xz} throughout the cross-sectional area of the constructs.

Differential scanning calorimetry (DSC)

Differential scanning calorimetry (DSC) (204 F1 Phoenix, Netzsch, Germany) was performed to determine the bound water content within hydrogels crosslinked in contact with PTFE or glass. GelMA/HAMA

hydrogels were prepared and photocrosslinked as described above, with samples allowed to swell overnight in PBS. Each sample was weighed (between 5–8 mg) for determination of equilibrium water content (EWC), then confined in a T-zero hermetic pan for DSC. Thermal profiles (n = 4–5 for all conditions) were acquired in a nitrogen atmosphere, with DSC performed at a heating rate of 10 °C per minute across a temperature range of −40 to 90 °C, in line with our previous studies[87,88]. The thermal profiles of the hydrogels were then used to determine the proportion of freezable water (W_f) and non-freezable bound water (W_{nfb}), with each expressed as a percentage of EWC (Fig. S1A–E, Supplementary Data).

$$W_f(\%) = \frac{\Delta H_f}{\Delta H_w} \times 100 \quad (3)$$

$$\mathrm{EWC}(\%) = \frac{W_s - W_d}{W_s} \times 100 \quad (4)$$

$$W_{nfb}(\%) = \mathrm{EWC} - W_f \quad (5)$$

In Eq. 3, ΔH_f is the enthalpy change in the DSC profile that corresponds to the melting of freezable water (integrated area in DSC), and ΔH_w is the enthalpy change of bulk water, which is 333.5 J g^{-1}. In Eq. 4, EWC is the equilibrium water content of the hydrogel, W_s is the sample weight after swelling, W_d is the dried sample weight; which allows W_{nfb} to be calculated, as in Eq. 5[87,88].

Additionally, independent DSC analyses were performed to obtain the thermal profiles of water interfaced with either glass or PTFE substrates. Thin circular substrate samples (4 mm diameter) of each material were acquired, with a 1 µL water droplet placed directly onto each of the substrate samples within T-zero hermetic pans for DSC. Differences in the thermal profiles of water when in contact with each substrate were used to determine W_f and W_{nfb} content, expressed as a percentage of EWC, for glass and PTFE substrates (Fig. S1F–I, Supplementary Data).

Human articular chondrocyte isolation and expansion

Human articular chondrocytes were isolated from macroscopically normal cartilage of the lateral femoral condyles of knee samples obtained from three donors (66 and 67 year old males, 56 year old female) undergoing total knee arthroplasty for osteoarthritis, as described elsewhere[9,17,57]. Following isolation, cells were expanded for 1–2 weeks to passage 1 on standard treated tissue culture plastic flasks (Nunc, ThermoFisher Scientific, QLD, Australia) in low-D-glucose chondrocyte basal medium (Dulbecco's modified Eagle's medium (DMEM) with 2 mM GlutaMAX™, 10 mM 4-(2-hydroxyethyl)-1-piperazineethanesulfonic acid (HEPES), 0.1 mM nonessential amino acids, 50 U mL^{-1} penicillin, 50 µg mL^{-1} streptomycin, 0.5 µg mL^{-1} amphotericin B (Fungizone®) (all Invitrogen, CA, USA), 0.4 mM L-proline and 0.1 mM L-ascorbic acid (both Sigma Aldrich, St. Louis, MO, USA)) supplemented with 10% foetal bovine serum (FBS) (Hyclone, Logan, UT, USA). All cell cultures/hydrogel constructs were incubated at 37 °C in a humidified 5% CO_2/95% air CO_2 incubator with the medium replaced every 3–4 days.

Chondrocyte encapsulation and redifferentiation

GelMA/HAMA hydrogel precursor solutions were prepared as described above. Passage 1 human articular chondrocytes were suspended in the hydrogel precursor solutions at 10 million cells per mL and photocrosslinked by exposure to 365 nm light within the aforementioned PTFE molds, as described above, in sterile conditions. Cell-hydrogel constructs were cultured in serum-free high-D-glucose basal chondrocyte medium (see above for composition) with ITS-G (100 × dilution), 1.25 mg mL^{-1} BSA, 0.1 µM dexamethasone (all Sigma Aldrich, St. Louis, MO, USA) and 10 ng mL^{-1} transforming growth factor beta 3 (TGF-β3) (GroPep, Adelaide, SA, Australia).

Biaxial mechanical stimulation of cell-hydrogel constructs

Constructs were either cultured under free swelling conditions for 28 days (static controls), or precultured for 14 days, followed by daily biaxial dynamic loading in a custom bioreactor[9] for 1 h at 1 Hz per day with a compressive strain of 30% of construct height and shear amplitude of 1 mm for another 14 days (3 donors, 2 constructs per donor for DNA and GAG analysis; 3 donors, 1 construct per donor for viability and immunofluorescence analysis; 3 donors, 2 constructs per donor for gene expression analysis). For all in vitro loading experiments, the compression setting of 30% replicated our previous studies indicating superior ECM production by cultured chondrocytes in comparison to 10% or 50% compression protocols[9]. In culture, hydrogel constructs were loosely confined beneath the PTFE loading pistons by laser-cut medical grade silicone rings (0.5 mm high, with a 5 mm × 5 mm hole in the center) fitted into the bottom of each well. A static offset compressive strain of approximately 10% was applied to ensure contact to all constructs. Thus, with the lower surface of each gel constrained within wells, the upper surface was the surface of interest in shear experiments for determination of frictional properties. The bioreactor system was maintained in a standard 5% CO_2/95% air CO_2 incubator at 37 °C for all experiments.

Cell viability assay

Live and dead chondrocytes were visualized with fluorescein diacetate (FDA) and propidium iodide (PI, both Sigma Aldrich, St. Louis, MO, USA), respectively. Constructs were washed in PBS at room temperature (RT), followed by incubation with 10 µg mL^{-1} FDA and 5 µg mL^{-1} PI in PBS for 3 min at RT, and then washed again in PBS. Z-stack fluorescence images were captured using a Carl Zeiss Axio microscope, and cell viability was quantified in at least 6 images from 3 biological replicates, respectively, using an ImageJ script (National Institutes of Health, USA). Cell viability is expressed as percentage of living to total cells.

Biochemical analysis

To analyze the DNA and glycosaminoglycan (GAG) content of cell-laden GelMA-HAMA constructs, samples were weighed and enzymatically digested in a two-step procedure by overnight incubation in phosphate-buffered EDTA (pH 7.1) containing 1 mg mL^{-1} hyaluronidase (Sigma Aldrich, St. Louis, MO, USA) at 37 °C, followed by addition of 0.5 mg mL^{-1} proteinase K (Invitrogen) and overnight incubation at 56 °C. DNA concentration in the digests was measured using the Quant-iT™ PicoGreen® dsDNA quantification assay (Invitrogen). GAG concentrations were measured using the dimethyl-methylene blue (DMMB) assay at pH 1.56 on day 28, to compare hydrogels cultured with and without mechanical loading.

Mechanical testing

The Young's moduli of constructs submerged in PBS at 37 °C were measured in unconfined compression tests using an Instron 5848 microtester equipped with a 5 N load cell (Instron, Melbourne, VIC, Australia). Constructs were compressed at 0.01 mm s^{-1} using a non-porous aluminium indenter and the Young's modulus was determined as the slope of the stress-strain curve from 10–15% strain, as we have described previously[17,83,84].

Gene expression analysis

Cell-laden hydrogel constructs were homogenized in TRIzol reagent (Invitrogen), and total RNA was isolated according to the manufacturer's instructions. Complementary DNA (cDNA) was synthesized using the SuperScript™ III First Strand Synthesis System (Invitrogen) with DNase and RNase digestions performed before and after cDNA synthesis, respectively. Quantitative reverse transcription real-time polymerase chain (qRT-PCR) was performed using SybrGreen® Mastermix (Invitrogen) and either a 7900HT fast real-time PCR system or QuantStudio™ 7 Flex Real-Time PCR system (Applied Biosystems). The cycle threshold (C_t) value of each gene was normalized to the geometric mean of the housekeeping genes *B2M* and *TBP* using the comparative C_t method ($2^{-\Delta Ct}$). The forward (F) and reverse (R) primer sequences (5′ → 3′) used for PCR were as follows: *ACAN*: F:GCCTGCGCTCCAATGACT, R: TAATGGAACACGATGCCTTTCA; *B2M*:F:ATGAGTATGCCTGCCGTGTGA, R:GGCATCTTCAAACCTC CATGATG; *COL1A1*: F:CAGCCGCTTCACCTACAGC, R:TTTTGTAT

TCAATCACTGTCTTGCC; *COL2A1*: F:GGCAATAGCAGGTTCACGTACA, R:CGATAACAGTCTTGCCCCACTT; *COL10A1*: F:ACCCAACACCAAGACACAGTTCT, R:TCTTACTGCTATACCTTTACTCTTTATGGTGTA; *MMP2*:F:CCGTCGCCCATCATCAA, R:AGATATTGCACTGCCAACTCT; *MMP13*: F:ACTTCACGATGGCATTGCTG, R:CATAATTTGGCCCAGGAGGA; *PRG4*: F:GAGTACCCAATCAAGGATTATCA, R:TCCATCTACTGGCTTACCATTGC; *TBP*: F:GAGCCAAGAGTGAAGAACAGTC, R:CATCACAGCTCCCCACCATATT.

Immunohistochemistry

Constructs were embedded in Optimal Cutting Temperature compound (OCT) (Sakura, Finetek, Tokyo, Japan), frozen, sectioned at a thickness of 10 µm, and air-dried. Sections were fixed with ice-cold acetone for 10 min, air-dried, rehydrated in 50 mM $BaCl_2$/100 mM Tris HCl buffer (pH 7.3) for 1 h, and incubated in 100 mM Tris HCl buffer (pH 7.3) for 5 min. Sections stained for collagen I and II were incubated with 0.1% w/v hyaluronidase (Sigma Aldrich, St. Louis, MO, USA) at 37 °C for 30 min for antigen retrieval. Primary antibodies for aggrecan (969D4D11, Invitrogen; 1:400 dilution in PBS with 2% donkey serum), collagen type I (I-8H5, MP Biomed, Solon, OH, USA; 1:300 dilution in PBS with 2% goat serum), and collagen type II (II-II6B3, Developmental Studies Hybridoma Bank (DSHB), Iowa City, IA, USA; 1:150 dilution in PBS with 2% goat serum) were applied overnight at 4 °C in a humidified chamber.

Secondary antibodies were diluted 1:150 in PBS with 2% goat/donkey serum and 5 µg mL^{-1} 4′, 6-diamidino-2-phenylindole (DAPI) (Invitrogen) and applied for 1 h in the dark (AlexaFluor® 488-labeled donkey anti-mouse, AlexaFluor® 488-labeled goat anti-mouse, AlexaFluor® 594-labeled goat anti-mouse; all Jackson ImmunoResearch, West Grove, PA, USA). A mouse IgG isotype control antibody (Jackson ImmunoResearch; 1:1000 dilution) and secondary antibody only were used as negative controls. Following two washing steps in PBS and drying, sections were mounted with ProLong Gold (Invitrogen) and imaged using a Zeiss Axio epifluorescence microscope (Zeiss Axio Imager 2). Integrated fluorescence density measurements were performed using ImageJ (National Institutes of Health, USA) on at least 6 immunofluorescence images from corresponding areas in the center and periphery of hydrogel constructs. Intensity values for ECM proteins were normalized to intensities obtained for DAPI staining to correct for differences in cell numbers between images.

Statistical analysis

Statistical analysis was performed using GraphPad Prism software (version 7–10; GraphPad, CA, USA) with a significance level of 0.05. One-way analysis of variance analyses (ANOVAs), with Tukey's multiple comparisons post-hoc tests with single pooled variance, were performed to investigate the effects of culture duration and culture condition on chondrocyte viability and gene expression, as well as total DNA and GAG content, wet weight, and Young's moduli of cell-laden constructs. For all ANOVAs, a confidence interval of 95% was used, with residuals assessed for normality with Shapiro-Wilk tests and Q-Q plots. Unpaired Student's t-tests were performed to investigate differences in AFM roughness and compression data. For all cell culture experiments performed, three donor populations of human articular chondrocytes were isolated and expanded, with 2 constructs per donor used for DNA and GAG analysis, 1 construct per donor for viability and immunofluorescence analyses, and 2 constructs per donor for gene expression analyses. Thus, given the low number of samples per donor, cell donor was not considered a factor in statistical analyses, with these grouped together. Statistical differences are indicated in figures using symbols (****$p < 0.0001$, ***$p < 0.001$, **$p < 0.01$, *$p < 0.05$).

Data availability

The data that support the findings of this study are available upon reasonable request from the authors.

Received: 28 October 2024; Accepted: 14 March 2025;
Published online: 27 March 2025

References

1. Adderley, N. & Sharma, S. Pleural Friction Rub, StatPearls Publishing (FL). http://europepmc.org/abstract/MED/30725803 (2023).
2. Moghani, T., Butler, J. P. & Loring, S. H. Determinants of friction in soft elastohydrodynamic lubrication. *J. Biomech.* **42**, 1069–1074 (2009).
3. Singh, A. et al. Enhanced lubrication on tissue and biomaterial surfaces through peptide-mediated binding of hyaluronic acid. https://doi.org/10.1038/NMAT4048 (2014).
4. Zhang, Y. S. & Khademhosseini, A. Advances in engineering hydrogels. *Science* **356**, eaaf3627 (2017).
5. Pereira, R. F., Barrias, C. C., Bártolo, P. J. & Granja, P. L. Cell-instructive pectin hydrogels crosslinked via thiol-norbornene photo-click chemistry for skin tissue engineering. https://doi.org/10.1016/j.actbio.2017.11.016 (2017).
6. Xavier, J. R. et al. Bioactive nanoengineered hydrogels for bone tissue engineering: a growth-factor-free approach. 45. https://doi.org/10.1021/nn507488s (2020).
7. Armstrong, J. P. K. et al. CommuniCation 1802649 (1 of 7) engineering anisotropic muscle tissue using acoustic cell patterning. https://doi.org/10.1002/adma.201802649 (2019).
8. Pahoff, S. et al. Effect of gelatin source and photoinitiator type on chondrocyte redifferentiation in gelatin methacryloyl-based tissue-engineered cartilage constructs †. *J. Mater. Chem. B* **7**, 1761 (2019).
9. Meinert, C., Schrobback, K., Hutmacher, D. W. & Klein, T. J. A novel bioreactor system for biaxial mechanical loading enhances the properties of tissue-engineered human cartilage. *Sci. Rep.* **7**, 1–14 (2017).
10. Butler, D. L., Goldstein, S. A. & Guilak, F. Functional tissue engineering: the role of biomechanics. *J. Biomech. Eng.* **122**, 570–575 (2000).
11. Bas, O. et al. Biofabricated soft network composites for cartilage tissue engineering. *Biofabrication* **9**, https://doi.org/10.1088/1758-5090/aa6b15 (2017).
12. Bin Imran, A. et al. ARTICLE extremely stretchable thermosensitive hydrogels by introducing slide-ring polyrotaxane cross-linkers and ionic groups into the polymer network. https://doi.org/10.1038/ncomms6124 (2014).
13. Gong, J. P. Friction and lubrication of hydrogels—its richness and complexity. *Soft Matter* **2**, 544–552 (2006).
14. Blum, M. M. & Ovaert, T. C. A novel polyvinyl alcohol hydrogel functionalized with organic boundary lubricant for use as low-friction cartilage substitute: synthesis, physical/chemical, mechanical, and friction characterization. *J. Biomed. Mater. Res. B Appl Biomater.* **100B**, 1755–1763 (2012).
15. Milner, P. E. et al. A low friction, biphasic and boundary lubricating hydrogel for cartilage replacement. *Acta Biomater.* **65**, 102–111 (2018).
16. Klein, J., Kumacheva, E., Mahalu, D., Perahia, D. & Fetters, L. J. Reduction of frictional forces between solid surfaces bearing polymer brushes. *Nature* **370**, 634–636 (1994).
17. Meinert, C. et al. Tailoring hydrogel surface properties to modulate cellular response to shear loading. *Acta Biomater.* **52**, https://doi.org/10.1016/j.actbio.2016.10.011 (2017).
18. Jhon, M. S. & Andrade, J. D. Water and hydrogels. *J. Biomed. Mater. Res.* **7**, 509–522 (1973).
19. Jungwirth, P. Biological water or rather water in biology? *J. Phys. Chem. Lett.* **6**, 2449–2451 (2015).
20. Tanaka, M., Hayashi, T. & Morita, S. The roles of water molecules at the biointerface of medical polymers. *Polym. J.* **45**, 701–710 (2013).
21. Dargaville, B. L. & Hutmacher, D. W. Water as the often neglected medium at the interface between materials and biology. *Nat. Commun.* **13**, https://doi.org/10.1038/s41467-022-31889-x (2022).
22. Gun'ko, V. M., Savina, I. N. & Mikhalovsky, S. V. Properties of water bound in hydrogels, Gels 3. https://doi.org/10.3390/gels3040037 (2017).

23. Vigata, M., Meinert, C., Bock, N., Dargaville, B. L. & Hutmacher, D. W. Deciphering the molecular mechanism of water interaction with gelatin methacryloyl hydrogels: role of ionic strength, ph, drug loading and hydrogel network characteristics. *Biomedicines* **9**, https://doi.org/10.3390/biomedicines9050574 (2021).
24. Gong, J. P. et al. Synthesis of hydrogels with extremely low surface friction. *J. Am. Chem. Soc.* **123**, 5582–5583 (2001).
25. Gong, J. P., Kii, A., Xu, J., Hattori, Y. & Osada, Y. A possible mechanism for the substrate effect on hydrogel formation. *J. Phys. Chem. B* **105**, 4572–4576 (2001).
26. Kurokawa, T., Gong, J. P. & Osada, Y. Substrate effect on topographical, elastic, and frictional properties of hydrogels. *Macromolecules* **35**, 8161–8166 (2002).
27. Levett, P. A. et al. A biomimetic extracellular matrix for cartilage tissue engineering centered on photocurable gelatin, hyaluronic acid and chondroitin sulfate. https://doi.org/10.1016/j.actbio.2013.10.005 (2014).
28. Levett, P. A., Hutmacher, D. W., Malda, J. & Klein, T. J. Hyaluronic acid enhances the mechanical properties of tissue-engineered cartilage constructs. *PLoS ONE* **9**, 113216 (2014).
29. Murakami, T., Yarimitsu, S., Nakashima, K., Sawae, Y. & Sakai, N. Influence of synovia constituents on tribological behaviors of articular cartilage. *Friction* **1**, 150–162 (2013).
30. Peng, M., Ping Gong, J. & Osada, Y. Substrate effect on the formation of hydrogels with heterogeneous network structure. *Chem. Rec.* **3**, 40–50 (2003).
31. Kii, A., Xu, J., Gong, J. P., Osada, Y. & Zhang, X. Heterogeneous polymerization of hydrogels on hydrophobic substrate. *J. Phys. Chem. B* **105**, 4565–4571 (2001).
32. Sophia Fox, A. J., Bedi, A. & Rodeo, S. A. The basic science of articular cartilage: structure, composition, and function. *Sports Health* **1**, 461–468 (2009).
33. Geurds, L., Xu, Y. & Stokes, J. R. Friction of lubricated hydrogels: influence of load, speed and lubricant viscosity. *Biotribology* **25**, 100162 (2021).
34. Chau, A. L., Urueña, J. M. & Pitenis, A. A. Load-independent hydrogel friction. *Biotribology* **26**, 100183 (2021).
35. Cuccia, N. L., Pothineni, S., Wu, B., Harper, J. M. & Burton, J. C. Pore-size dependence and slow relaxation of hydrogel friction on smooth surfaces. *Proc. Natl Acad. Sci. USA* **117**, 11247–11256 (2020).
36. Dunn, A. C. et al. Lubricity of surface hydrogel layers. *Tribol. Lett.* **49**, 371–378 (2013).
37. Meier, Y. A., Zhang, K., Spencer, N. D. & Simic, R. Linking friction and surface properties of hydrogels molded against materials of different surface energies. *Langmuir* **35**, 15805–15812 (2019).
38. Kim, J. & Dunn, A. C. Soft hydrated sliding interfaces as complex fluids. *Soft Matter* **12**, 6536–6546 (2016).
39. Kim, J. & Dunn, A. C. Thixotropic mechanics in soft hydrated sliding interfaces. *Tribol. Lett.* **66**, 102 (2018).
40. Simič, R. & Spencer, N. D. Controlling the friction of gels by regulating interfacial oxygen during polymerization. *Tribol. Lett.* **69**, 86 (2021).
41. Simič, R., Mandal, J., Zhang, K. & Spencer, N. D. Oxygen inhibition of free-radical polymerization is the dominant mechanism behind the "mold effect" on hydrogels. *Soft Matter* **17**, 6394–6403 (2021).
42. Ong, L. J. Y. et al. Localized oxygen control in a microfluidic osteochondral interface model recapitulates bone–cartilage crosstalk during osteoarthritis. *Adv. Funct. Mater.* **34**, 2315608 (2024).
43. Khorshidi, S. & Karkhaneh, A. A hydrogel/particle composite with gradient in oxygen releasing microparticle for oxygenation of the cartilage-to-bone interface: modeling and experimental viewpoints. *Mater. Sci. Eng. C.* **118**, 111522 (2021).
44. Jahn, S., Seror, J. & Klein, J. Lubrication of articular cartilage. *Annu Rev. Biomed. Eng.* **18**, 235–258 (2016).
45. Waldman, S. D., Spiteri, C. G., Grynpas, M. D., Pilliar, R. M. & Kandel, R. A. Long-term intermittent shear deformation improves the quality of cartilaginous tissue formed in vitro. *J. Orthop. Res.* **21**, 590–596 (2003).
46. Jin, M., Frank, E. H., Quinn, T. M., Hunziker, E. B. & Grodzinsky, A. J. Tissue shear deformation stimulates proteoglycan and protein biosynthesis in bovine cartilage explants. *Arch. Biochem. Biophys.* **395**, 41–48 (2001).
47. Coles, J. M. et al. Loss of cartilage structure, stiffness, and frictional properties in mice lacking PRG4. *Arthritis Rheum.* **62**, 1666–1674 (2010).
48. Teeple, E. et al. Coefficients of friction, lubricin, and cartilage damage in the anterior cruciate ligament-deficient guinea pig knee. *J. Orthop. Res.* **26**, 231–237 (2008).
49. Elsaid, K. A., Jay, G. D., Warman, M. L., Rhee, D. K. & Chichester, C. O. Association of articular cartilage degradation and loss of boundary-lubricating ability of synovial fluid following injury and inflammatory arthritis. *Arthritis Rheum.* **52**, 1746–1755 (2005).
50. Roos, E. M. Joint injury causes knee osteoarthritis in young adults. *Curr. Opin. Rheumatol.* **17**, https://journals.lww.com/co-rheumatology/fulltext/2005/03000/joint_injury_causes_knee_osteoarthritis_in_young.16.aspx (2005).
51. Wong, B. L. et al. Biomechanics of cartilage articulation: effects of lubrication and degeneration on shear deformation. *Arthritis Rheum.* **58**, 2065–2074 (2008).
52. Bian, L. et al. Dynamic mechanical loading enhances functional properties of tissue-engineered cartilage using mature canine chondrocytes. *Tissue Eng. Part A* **16**, 1781–1790 (2009).
53. Paul, S. et al. Photo-cross-linkable, injectable, and highly adhesive GelMA-Glycol Chitosan hydrogels for cartilage repair. *Adv. Health. Mater.* **2302078**, 1–19 (2023).
54. Paul, S. et al. GelMA-glycol chitosan hydrogels for cartilage regeneration: the role of uniaxial mechanical stimulation in enhancing mechanical, adhesive, and biochemical properties. *APL Bioeng.* **7**, https://doi.org/10.1063/5.0160472 (2023).
55. Pahoff, S. et al. Effect of gelatin source and photoinitiator type on chondrocyte redifferentiation in gelatin methacryloyl-based tissue-engineered cartilage constructs. *J. Mater. Chem. B* **7**, 1761–1772 (2019).
56. Visser, J. et al. Reinforcement of hydrogels using three-dimensionally printed microfibres. *Nat. Commun.* **6**, 6933 (2015).
57. Klein, T. J. et al. Long-term effects of hydrogel properties on human chondrocyte behavior. *Soft Matter* **6**, 5175–5183 (2010).
58. Nam, Y., Rim, Y. A., Lee, J. & Ju, J. H. Current therapeutic strategies for stem cell-based cartilage regeneration. *Stem Cells Int.* **2018**, 8490489 (2018).
59. Vogel, C. & Marcotte, E. M. Insights into the regulation of protein abundance from proteomic and transcriptomic analyses. *Nat. Rev. Genet.* **13**, 227–232 (2012).
60. Liu, Y., Beyer, A. & Aebersold, R. On the dependency of cellular protein levels on mRNA abundance. *Cell* **165**, 535–550 (2016).
61. Maier, T., Güell, M. & Serrano, L. Correlation of mRNA and protein in complex biological samples. *FEBS Lett.* **583**, 3966–3973 (2009).
62. Guilak, F., Nims, R. J., Dicks, A., Wu, C.-L. & Meulenbelt, I. Osteoarthritis as a disease of the cartilage pericellular matrix. *Matrix Biol.* **71–72**, 40–50 (2018).
63. Little, C. B. & Fosang, A. J. Is cartilage matrix breakdown an appropriate therapeutic target in osteoarthritis–insights from studies of aggrecan and collagen proteolysis? *Curr. Drug Targets* **11**, 561–575, https://api.semanticscholar.org/CorpusID:23840174 (2010).
64. Makris, E. A., Gomoll, A. H., Malizos, K. N., Hu, J. C. & Athanasiou, K. A. Repair and tissue engineering techniques for articular cartilage. *Nat. Rev. Rheumatol.* **11**, 21–34 (2015).
65. Eshed, I. et al. Assessment of cartilage repair after chondrocyte transplantation with a fibrin-hyaluronan matrix – Correlation of

morphological MRI, biochemical T2 mapping and clinical outcome. *Eur. J. Radio.* **81**, 1216–1223 (2012).
66. Nehrer, S., Chiari, C., Domayer, S., Barkay, H. & Yayon, A. Results of chondrocyte implantation with a fibrin-hyaluronan matrix: a preliminary study. *Clin. Orthop. Relat. Res*. 1849–1855. https://doi.org/10.1007/s11999-008-0322-4 (2008).
67. Zeifang, F. et al. Autologous chondrocyte implantation using the original periosteum-cover technique versus matrix-associated autologous chondrocyte implantation: a randomized clinical trial. *Am. J. Sports Med.* **38**, 924–933 (2009).
68. Ossendorf, C. et al. Treatment of posttraumatic and focal osteoarthritic cartilage defects of the knee with autologous polymer-based three-dimensional chondrocyte grafts: 2-year clinical results. *Arthritis Res. Ther.* **9**, R41 (2007).
69. Schneider, U. et al. A prospective multicenter study on the outcome of Type I Collagen Hydrogel–Based Autologous Chondrocyte Implantation (CaReS) for the repair of articular cartilage defects in the knee. *Am. J. Sports Med.* **39**, 2558–2565 (2011).
70. Petri, M. et al. CaReS® (MACT) versus microfracture in treating symptomatic patellofemoral cartilage defects: a retrospective matched-pair analysis. *J. Orthop. Sci.* **18**, 38–44 (2013).
71. Saris, D. B. F. et al. Characterized chondrocyte implantation results in better structural repair when treating symptomatic cartilage defects of the knee in a randomized controlled trial versus microfracture. *Am. J. Sports Med.* **36**, 235–246 (2008).
72. Bartlett, W. et al. Autologous chondrocyte implantation versus matrix-induced autologous chondrocyte implantation for osteochondral defects of the knee. *J. Bone Jt. Surg. Br.* **87-B**, 640–645 (2005).
73. Almany, L. & Seliktar, D. Biosynthetic hydrogel scaffolds made from fibrinogen and polyethylene glycol for 3D cell cultures. *Biomaterials* **26**, 2467–2477 (2005).
74. Wang, D.-A. et al. Multifunctional chondroitin sulphate for cartilage tissue–biomaterial integration. *Nat. Mater.* **6**, 385–392 (2007).
75. Sharma, B. et al. Human cartilage repair with a photoreactive adhesive-hydrogel composite. *Sci. Transl. Med.* **5**, 167ra6 (2013).
76. Ji, X. et al. Cartilage repair mediated by thermosensitive photocrosslinkable TGFβ1-loaded GM-HPCH via immunomodulating macrophages, recruiting MSCs and promoting chondrogenesis. *Theranostics* **10**, 2872–2887 (2020).
77. Kurian, A. G., Singh, R. K., Patel, K. D., Lee, J. H. & Kim, H. W. Multifunctional GelMA platforms with nanomaterials for advanced tissue therapeutics. *Bioact. Mater.* **8**, 267–295 (2022).
78. Bryant, S. J., Nuttelman, C. R. & Anseth, K. S. Cytocompatibility of UV and visible light photoinitiating systems on cultured NIH/3T3 fibroblasts in vitro. *J. Biomater. Sci. Polym. Ed.* **11**, 439–457 (2000).
79. de Gruijl, F. R. Photocarcinogenesis: UVA vs UVB. *Methods Enzymol*. 359–366. https://doi.org/10.1016/S0076-6879(00)19035-4 (2000).
80. Fairbanks, B. D., Schwartz, M. P., Bowman, C. N. & Anseth, K. S. Photoinitiated polymerization of PEG-diacrylate with lithium phenyl-2,4,6-trimethylbenzoylphosphinate: polymerization rate and cytocompatibility. *Biomaterials* **30**, 6702–6707 (2009).
81. Lin, H., Cheng, A. W.-M., Alexander, P. G., Beck, A. M. & Tuan, R. S. Cartilage tissue engineering application of injectable gelatin hydrogel with in situ visible-light-activated gelation capability in both air and aqueous solution. *Tissue Eng. Part A* **20**, 2402–2411 (2014).
82. Bas, O. et al. Rational design and fabrication of multiphasic soft network composites for tissue engineering articular cartilage: a numerical model-based approach. https://doi.org/10.1016/j.cej.2018.01.020 (2018).
83. Loessner, D. et al. Functionalization, preparation and use of cell-laden gelatin methacryloyl-based hydrogels as modular tissue culture platforms. *Nat. Protoc.* **11**, 727–746 (2016).
84. Schuurman, W. et al. Gelatin-methacrylamide hydrogels as potential biomaterials for fabrication of tissue-engineered cartilage constructs. *Macromol. Biosci.* **13**, 551–561 (2013).
85. Smeds, K. A. et al. Erratum: photocrosslinkable polysaccharides for in situ hydrogel formation (Journal of Biomedical Materials Research (2000) 54 (115−121)). *J. Biomed. Mater. Res.* **55**, 254 (2001).
86. Katta, J., Pawaskar, S. S., Jin, Z. M., Ingham, E. & Fisher, J. Effect of load variation on the friction properties of articular cartilage. In *Proc. Institution of Mechanical Engineers*, *Part J: Journal of Engineering Tribology*. 175–181. https://doi.org/10.1243/13506501JET240 (2007).
87. Yang, X., Dargaville, B. L. & Hutmacher, D. W. Elucidating the molecular mechanisms for the interaction of water with polyethylene glycol-based hydrogels: Influence of ionic strength and gel network structure. *Polymers* **13**, https://doi.org/10.3390/polym13060845 (2021).
88. Chang, C. W., Dargaville, B. L., Momot, K. I. & Hutmacher, D. W. An investigation of water status in gelatin methacrylate hydrogels by means of water relaxometry and differential scanning calorimetry. *J Mater Chem B*. https://doi.org/10.1039/d4tb00053f (2024).

Acknowledgements

This work was supported by funding from the Australian Research Council (ARC) – Future Fellowship awarded to T.J. Klein; Discovery Project grants awarded to T.J. Klein and D.W. Hutmacher; and through the ARC Training Centre in Additive Biomanufacturing, and the Max Planck Queensland Centre (MPQC). We also acknowledge funding awarded to C. Meinert via an ASBTE International Lab Travel Award which facilitated visitation M.M. Stevens' lab at Imperial College, London; and funding awarded to A. Weekes via a QUT MMPE Early Career Researcher seed grant. A. Gelmi acknowledges support from the European Union's Horizon 2020 Research and Innovation Programme through the Marie Skłodowska-Curie Individual Fellowship "RAISED" under grant agreement no. 660757. M.M. Stevens acknowledges support from the Wellcome Trust Senior Investigator Grant (098411/Z/12/Z). The data reported were obtained using the resources of the QUT Central Analytical Research Facility (CARF). Open access publishing facilitated by QUT through the Council of Australian University Librarians (CAUL) agreement.

Author contributions

T.J. Klein, D.W. Hutmacher, K. Schrobback, and M.M. Stevens conceptualized and supervised the research project; C. Meinert, A. Weekes, C. Chang, and A. Gelmi designed and performed experiments, collected and analysed data; C. Meinert & A. Weekes wrote the manuscript; all authors reviewed findings, edited and revised the manuscript and revisions; C. Meinert & A. Weekes contributed equally to this work.

Competing interests

C. Meinert, T.J. Klein, and D.W. Hutmacher are co-founders and shareholders of Gelomics Pty Ltd. C. Meinert is also the Chief Executive Officer and an Executive Director of Gelomics Pty Ltd. T.J. Klein, D.W. Hutmacher and M.M. Stevens serve on the Scientific Advisory Board of Gelomics Pty Ltd. M.M. Stevens has invested in, consults for (or is on scientific advisory boards or boards of directors) and conducts sponsored research funded by companies related to the biomaterials field; has filed patent applications related to biomaterials; and has co-founded companies in the biomaterials field.

Ethics approval

Ethical approval was granted for this research from the Queensland University of Technology Human Research Ethics Committee (EC00171) and the Prince Charles Hospital Human Research Ethics Committee (EC00168) (both Brisbane, Australia), and written informed consent was obtained from donors for use of tissue samples. All experiments were performed in accordance with the National Health and Medical Research Council (NHMRC) guidelines.

Additional information

Supplementary information The online version contains supplementary material available at https://doi.org/10.1038/s43246-025-00781-8.

Correspondence and requests for materials should be addressed to Travis J. Klein.

Peer review information *Communications Materials* thanks Ana Ferreira, Jeanne E. Barthold, and Anna Trengove for their contribution to the peer review of this work. Primary Handling Editors: Steven Caliari and Jet-Sing Lee. [A peer review file is available.].